JOURNAL OF THE ROYAL SOCIETY Interface
J. R. Soc. Interface (2008) **5**, 477–481
doi:10.1098/rsif.2007.1249
Published online 27 November 2007

REPORT

X-ray colour imaging

R. J. Cernik*, K. H. Khor and C. Hansson

School of Materials, University of Manchester, Manchester M1 7HS, UK

A prototype X-ray colour imaging system has been assembled using the principle of tomographic energy-dispersive diffraction imaging (TEDDI). The new system has been tested using samples of nylon-6, aluminium powder and deer antler bone. Non-destructive three-dimensional images of the test objects have been reconstructed on a 300 μm scale with an associated diffraction pattern at each voxel. In addition, the lattice parameters of the polycrystalline material present in the sampled voxels have been determined using full pattern refinement methods. The use of multiple diffracted parallel colour X-ray beams has allowed simultaneous spatially resolved data collection across a plane of the sample. This has simplified the sample scan motion and has improved data collection times by a factor scaling with the number of detector pixels. The TEDDI method is currently limited to thin samples (approx. 1–2 mm) with light atoms owing to the very low detection efficiency of the silicon detector at X-ray energies above 25 keV. We describe how these difficulties can be removed by using semiconductor detectors made from heavier atomic material.

Keywords: imaging; synchrotron; energy dispersive diffraction

1. INTRODUCTION

X-rays currently provide three-dimensional density contrast images for a wide range of applications most commonly encountered in the fields of medicine and security in the form of spiral CT or baggage scanners. However, the information carried by different wavelength (or colour) X-rays is rarely used in these modalities. This information is potentially very useful because it can be used to identify tissue types (Harding *et al.* 1990), strain distributions in whole engineered components or the presence of illegal substances in luggage (McGann *et al.* 1993). A full X-ray colour imaging modality needs spectroscopy-grade pixellated solid-state detectors and corresponding high aspect ratio collimators which have hitherto not been available. We show for the first time how the necessary energy-sensitive detector and collimator arrays can produce genuine three-dimensional X-ray 'colour' images with associated energy-dispersive diffraction (EDD) patterns at each voxel for a range of samples across scientific disciplines.

The underlying principle of tomographic energy-dispersive diffraction imaging (TEDDI) has been described before using a single Ge solid-state detector scanning the sample in three dimensions on a 20 μm scale (Hall *et al.* 1998; Barnes *et al.* 2000). This is very time consuming, often requiring 20 hours or more to complete. The developments we describe here have enabled us to obtain much faster X-ray colour images with one simple scan motion while delivering a lower dose of X-rays to the subject under investigation.

The imaging geometry of the TEDDI X-ray colour imaging system is illustrated in figure 1*a*. A polychromatic X-ray beam from a synchrotron or X-ray tube is incident upon the study object. The X-rays are scattered into a set of highly parallel collimator apertures each with an aspect ratio of 4000 : 1 (Tunna *et al.* 2006) or higher. The X-ray beams that pass through the collimator apertures are recorded by an energy-sensitive pixellated detector (Seller *et al.* 1998). The tomographic element of the scattering process is enabled because a specific gauge volume (shown shaded in figure 1) is sampled by the intersection of the incident and diffracted beams. At the low 2θ angles necessary for observing diffraction patterns at high energy, the spatial resolution along the beam direction may be 10 times lower than the collimator aperture. An alternative scattering geometry is shown in figure 1*b*, but this is possible only with thin samples and a box beam illuminating the sample. The gauge volume is dictated by the sample thickness and the collimator geometry gives vertical rather than depth spatial separation. Despite this spatial limitation the method provides very simple and informative images.

2. RESULTS

We present here the first results in X-ray colour imaging using our prototype collimator and detector array system. The detector consists of a 16×16 array of energy-sensitive pixel elements (300×300 μm) and a corresponding 16×16 array of 50 μm diameter collimators. Each pixel records the EDD pattern from the intersection volume in the sample. This can be used to identify the material present at that point in the sample. The total scattering count gives an image of the whole sample which is proportional to the density contrast. In addition, the scattered spectra contain X-ray fluorescence (XRF) information that can also be used for material characterization. Figure 2*a* shows the experimental system on beamline 7.6 of the SRS at Daresbury Laboratory. The Si-pixellated detector was carefully aligned to our very fine tolerance laser-drilled X-ray collimators. A thin polymer sheet with a cross test mark (figure 2*b*) was placed in a 5×5 mm X-ray beam as shown in figure 1*b*. The total scattering from each pixel is shown in figure 2*c*, the intensity is false coloured, the lighter the colour the greater the count rate. Figure 2*d* shows the individual energy-dispersive X-ray scattering pattern from each pixel. There is no scattering where the polymer material has been

*Author for correspondence (r.cernik@manchester.ac.uk).

Received 2 October 2007
Accepted 8 November 2007

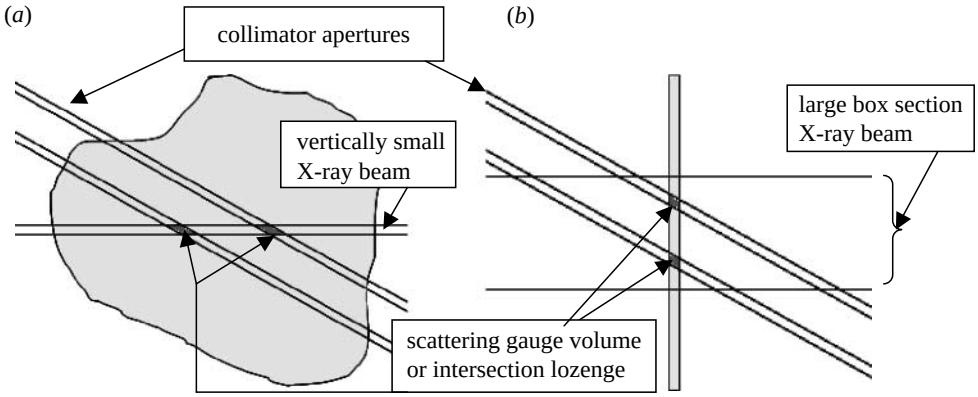

Figure 1. (*a*) A vertically thin polychromatic beam incident on a thick sample. Two of the collimator apertures are shown. The scattering is measured only where the incident beam intersects with the projected collimator aperture (shaded), thus giving spatial resolution to the sample. (*b*) A similar effect but with a large box beam and a very thin sample. Note the direction of special resolution is now vertical.

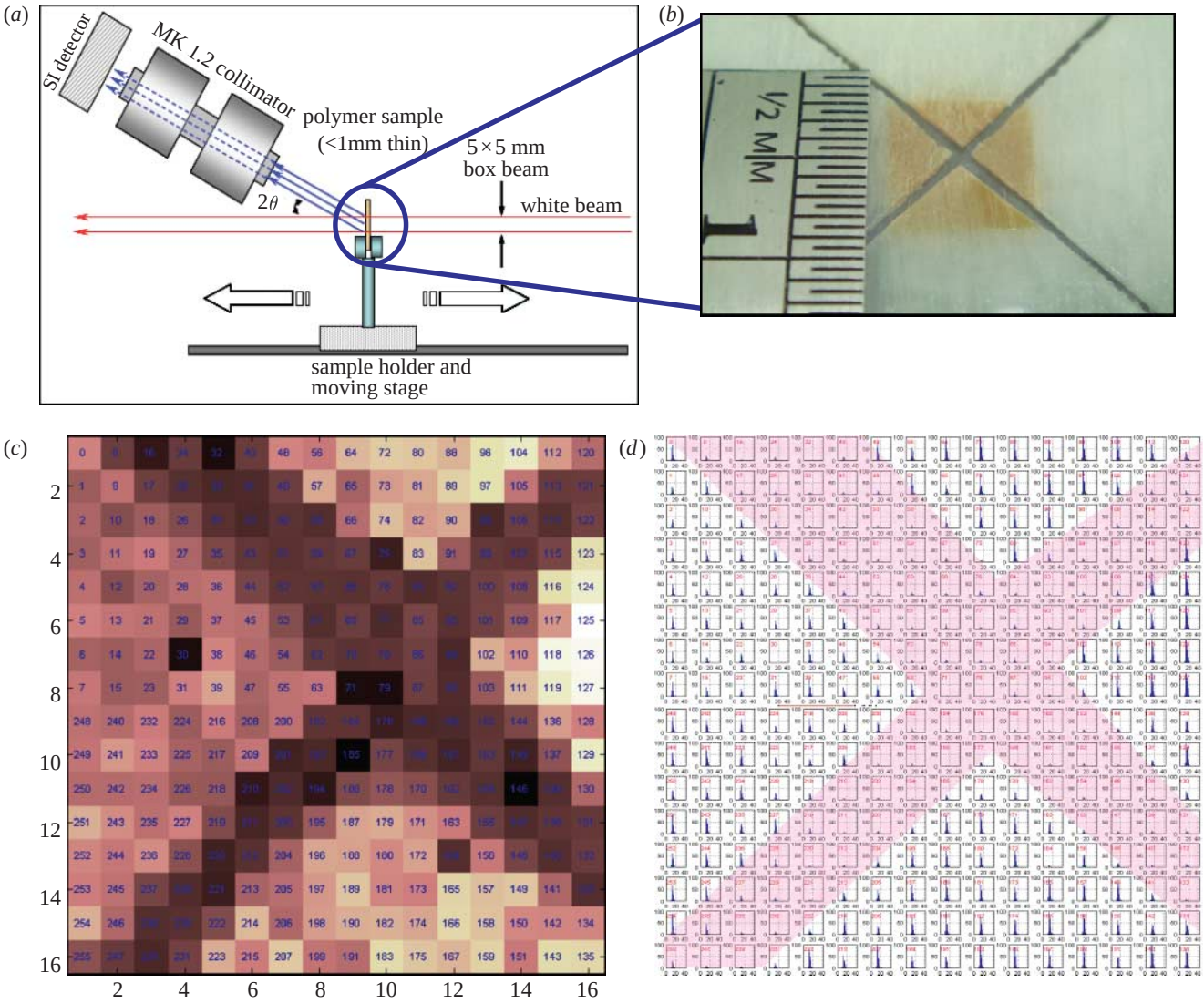

Figure 2. (*a*) Thin polymer sample mounted in the X-ray beam with the collimator and detector array inclined at an angle of 22° to the horizontal. (*b*) Polymer sample with a test cross cut out, the beam discolouration can be seen. (*c*) The TEDDI image from the polymer sample (lighter colour indicates higher photon count). (*d*) The energy-dispersive diffraction patterns recorded at each pixel. Note the absence of scattering where the material has been removed (shaded).

removed to form the test cross mark. The remainder of the pixels clearly display an energy-dispersive X-ray diffraction pattern. This pattern can be used in a number of ways; for example, to identify the material at the gauge volume position in the sample against a set of stored spectra, refine lattice parameters to determine strain distributions or identify materials based on characteristic fluorescence. This information is present

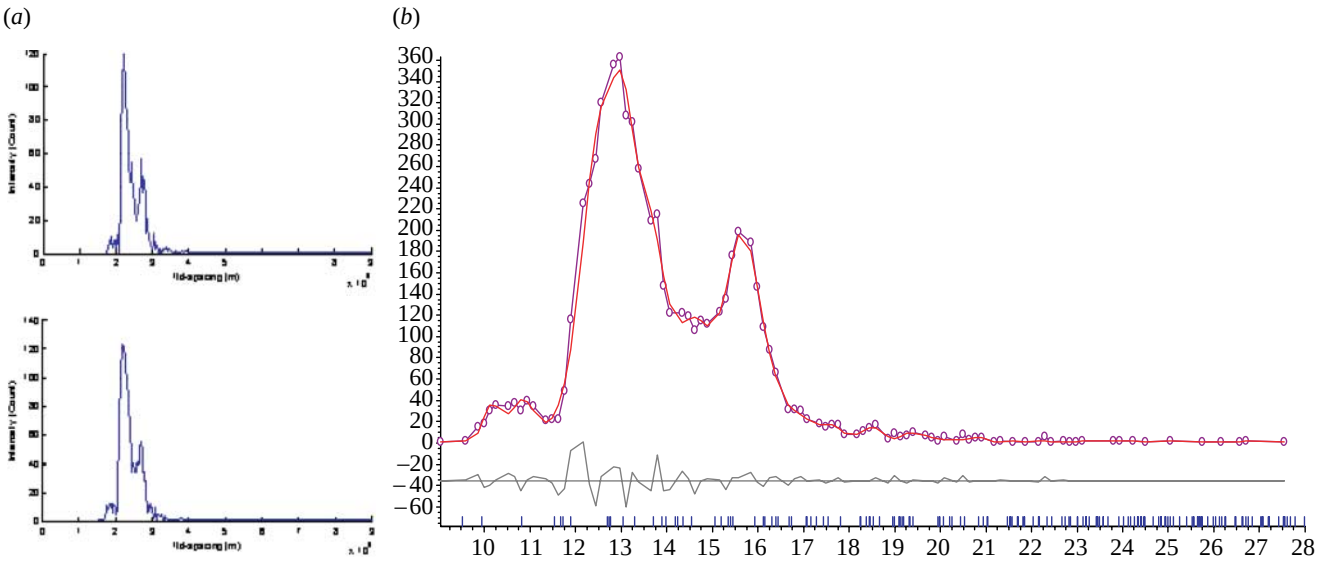

Figure 3. (*a*) Two typical diffraction patterns from different pixels obtained from a thin polymer sample later identified as nylon-6. (*b*) A lattice parameter refinement of the nylon-6 sample where the observed data points (I_{obs}) are fitted with the smooth red line (I_{calc}). The I_{obs}–I_{calc} curve is shown in grey together with tick marks at the expected Bragg peak positions (blue). The refinement converged to a χ^2 of 1.45 with lattice parameter errors in the second decimal place.

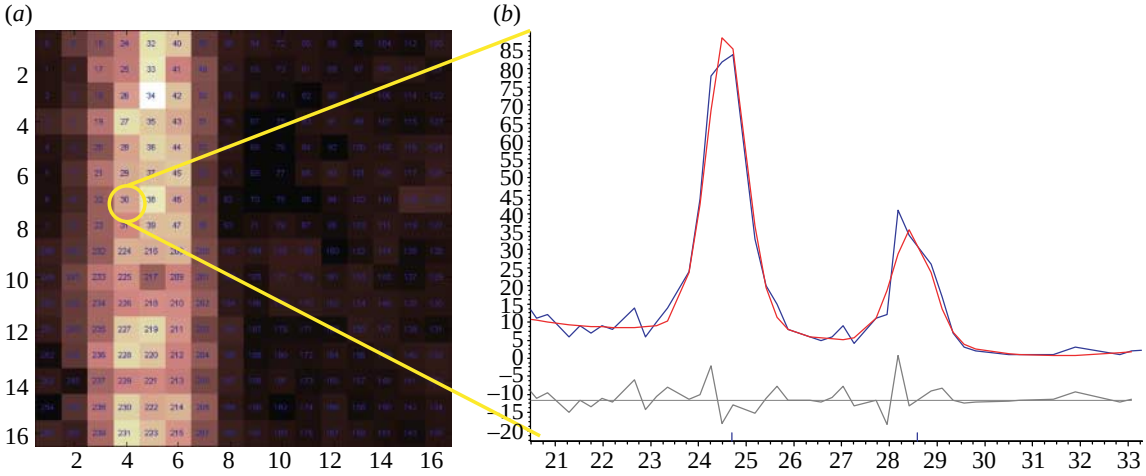

Figure 4. (*a*) A TEDDI image of a slice through a thin aluminium pressed powder sample. (*b*) The energy-dispersive spectra from a typical pixel have been refined. Although the observed data (blue) are of poor statistical quality, a good fit (red) was obtained with $\chi^2 = 0.94$ and $a = 4.0497(38)$ Å.

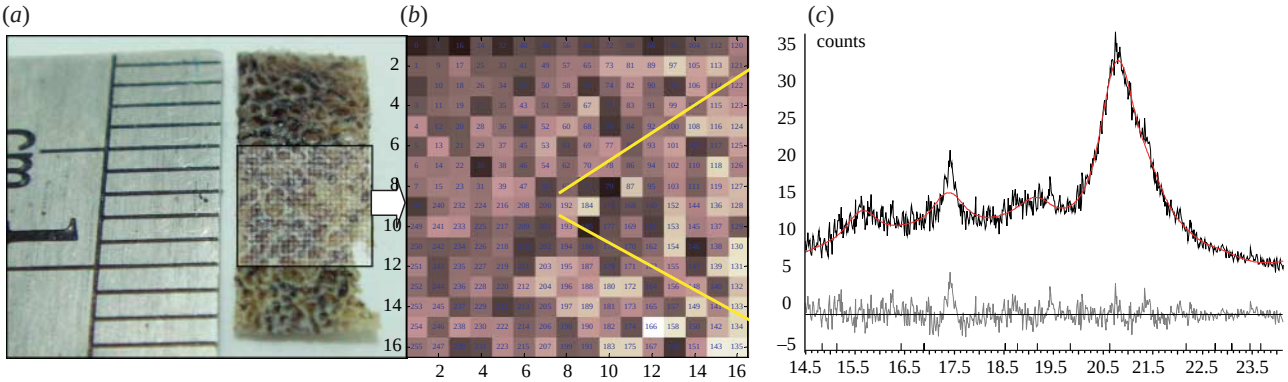

Figure 5. (*a*) A 1 mm thick section of deer antler bone together with the 5 mm^2 area investigated using rapid TEDDI. (*b*) The corresponding rapid TEDDI image. (*c*) A diffraction pattern from one of the pixels together with output of a refinement of the known hydroxyapatite lattice parameters.

in each pixel, it is the choice of the experimenter to decide which to analyse.

Figure 3*a* shows the EDD patterns from two pixels in the detector array. The patterns are similar but not identical. Local variations in structure and preferred orientation are largely responsible for these differences. A lattice parameter refinement was carried out using Topas (Kern & Coelho 1998) and despite the limited statistical quality in each pixel due to the low count rate a χ^2 of 1.45 was achieved with the possible space groups $P21$, $P21/m$ or $P21/c$, $a=7.058(50)$, $b=10.679(36)$, $c=17.83(15)$ Å and $\beta=68.4(21)°$ corresponding to the structure of nylon-6. This was later confirmed by collecting an FTIR spectrum and referring the result to that of nylon-6 stored in the Hummel Polymer Library (A. Wilkinson *et al.* 2007, private communication). The accuracy of the lattice parameters from the Topas refinement is lower than that expected from traditional powder measurements, occurring in this case to the second decimal place; however, detector efficiency improvements will alleviate this problem. The intensity variations due to local structural differences can be treated qualitatively to give information on grain clustering (Cernik *et al.* 2007). However, the integrated intensities are not sufficiently reliable to enable structure determination or full Rietveld refinement.

There is a great deal of interest within engineering communities in the non-destructive determination of residual stresses in manufactured components especially in critical areas such as aircraft wings and engine casings. The TEDDI system can be used for strain scanning whole fabricated components in the automotive or aerospace industries, however, even though we are currently limited to light alloys. Figure 4*a* shows the image of a thin sheet of pressed aluminium powder. The pixels are false coloured in the same way as in figure 2. The EDD pattern is shown alongside with a lattice parameter refinement. Two peaks are visible: the (1 1 1) and the (0 0 2). Despite the limited statistical quality, a successful lattice parameter refinement was possible with $\chi^2=0.94$ and $a=4.0497(38)$ Å. This level of accuracy could be used, for example, to map the strain distribution across a weld.

The TEDDI method is highly applicable to biomaterials with the possibility of specific tissue identification. As an example we studied a section of deer antler bone with a network of trabeculae shown in figure 5*a*. The corresponding rapid TEDDI image is shown in figure 5*b*. The EDD pattern in this case was sufficiently well resolved to identify the sample as one of the hydroxyapatites but not to distinguish further between types. Figure 5*c* shows the diffraction pattern and the full pattern fit. The main observed peaks in the spectrum are the 1 2 1; 1 1 2 and 0 3 0 characteristic of the apatites (Kay *et al.* 1964). The refinement gave $a=9.323(9)$, $c=7.425$ Å in the space group $P6_3/m$.

3. CONCLUSIONS

The prototype TEDDI system has significant potential as a multidisciplinary imaging tool. However, our samples were limited in physical size and counting statistics by the low quantum counting efficiency of silicon detectors at high X-ray energies. In our case this was less than 1% above 25 keV. This single factor was responsible for the undesirably long data collection times. These were significantly shorter than the 20 hours point by point scans previously described (Barnes *et al.* 2000) but were typically 2–3 hours. This would allow the study of a thin alloy sample for use in aerospace engineering applications, but would not be suitable for studying a biopsy sample owing to radiation damage problems. We are currently developing new, high purity, high atomic weight semiconductor detector materials[1] that will remove this difficulty. Cadmium zinc telluride area detectors will be used to replace silicon, these have been shown to be 60% efficient at 100 keV for 500 µm thick material. We have designed 2 mm thick active sensors and expect data collection times to drop by two orders of magnitude giving a 300 µm resolution reconstruction of a 2 cm^3 biological sample in 180 s.

We anticipate that one of the main uses of the TEDDI method in the life sciences will be in distinguishing normal from abnormal tissue types. Geraki *et al.* (2002, 2004) have developed a synchrotron-based method combining XRF and EDD to examine biopsies of healthy and cancerous breast tissue. The XRF was used to examine the differential accumulation of iron, copper, zinc and potassium between the abnormal and diseased tissue while the EDD data were used to evaluate the quantities of adipose and fibrous tissue present. The shape and distribution of the EDD spectra from the healthy cells are quite different from those of the tumour cells and could be easily separated out by automatic sampling methods. Their XRF analysis revealed that all four elements are found in elevated levels in the tumour specimens. The rapid TEDDI method described in this paper gives simultaneous fluorescence and diffraction measurements which will greatly facilitate this type of biopsy sampling. Lewis *et al.* (2000) have described the structural changes in collagen associated with cancerous tissue. These features were measured with small angle scattering over a size range of 75–1390 Å. Structural features of these dimensions cannot be measured with TEDDI since the diffraction angles are practically too small. However, it is quite possible with low detector angles and energies in the region of 20 keV to probe structures on a 30 Å scale. The usefulness of this was described by Castro *et al.* (2005) with regard to the analysis of uterine, kidney and breast duct carcinoma biopsies. The observed structural changes in the first case were too subtle for the TEDDI method to distinguish without improvements to the energy resolution. However, the structural changes measured for the last two cases are of the correct order or magnitude to be observed by the rapid TEDDI system.

The TEDDI system generates new imaging possibilities in the physical sciences including the analysis of strain distributions in fabricated components for the

[1]HEXITEC project funded by EPSRC http://www.hexitec.co.uk/.

aerospace industry; the identification of oil- and gas-bearing seams in geological core samples and for security scanning at airports. In these cases the radiation dosages are less critical. However, there is still a need to use more efficient detector material and higher energy X-rays owing to the need to study fabricated or machined components with large volumes. The result has exciting implications for non-destructive strain scanning of assembled light alloy components because an image, structure variation and strain distribution can be obtained simultaneously. This development will significantly enhance the type of strain scanning studies with whole fabricated components such as those described by Korsunsky *et al.* (2002). Further examples of the point by point scanning TEDDI method were described by Harding & Schreiber (1999) with reference to the security industry and the need to identify specific substances inside large containers. Energy-dispersive spectra from a variety of samples were demonstrated to be quite clearly distinct and identifiable despite rather poor counting statistics. The range of samples unambiguously identified from their diffraction patterns included semtex, cocaine and heroin.

It would be highly desirable to develop laboratory-based TEDDI systems for medical, security and process control applications, but it is probable that the higher energy applications for engineering or earth sciences will need synchrotron radiation. However, Honemaki *et al.* (1990) made a comparison of the X-ray flux available for sealed tube, rotating anode and synchrotron sources, demonstrating that if a large opening angle can be accepted (as in the case of TEDDI) the fluxes at the samples can be very similar. We therefore conclude that the X-ray flux available from a tungsten sealed source tube with a short source to sample distance and a wide opening angle will be very similar to the limited photon flux of beamline 7.6 at Daresbury Laboratory. With better detector efficiency we could expect the TEDDI images to be produced from a laboratory-based source which is very important if biopsy screening is to become viable.

We have demonstrated for the first time that our TEDDI imaging system can deliver spatially resolved images with one very simple scanning motion. These images fully use the multiwavelength, or colour, information present in the incident X-ray beam. This gives three-dimensional density contrast images and structural information at each voxel point. The rapid TEDDI system forms the basis of a powerful new modality in X-ray imaging.

We would like to thank the EPSRC and CCLRC for research support and access to the research facilities.

REFERENCES

Barnes, P. *et al.* 2000 Time- and space-resolved dynamic studies on ceramic and cementitious materials. *J. Synchrotron Radiat.* **7(Pt 3)**, 167–177. (doi:10.1107/S0909049500003137)

Castro, C. R. F., Barroso, R. C. & Lopes, R. T. 2005 Scattering signatures from some human tissues using synchrotron radiation. *X-ray Spectrom.* **34**, 477–480. (doi:10.1002/xrs.862)

Cernik, R. J., Freer, R., Leach, C., Mongkolkachit, C., Barnes, P., Jacques, S., Pile, K. & Wander, A. 2007 Direct correlation between ferrite microstructure and electrical resistivity. *J. Appl. Phys.* **101**, 104 912. (doi:10.1063/1.2735400)

Geraki, K., Farquharson, M. J. & Bradley, D. A. 2002 Concentrations of Fe, Cu and Zn in breast tissue; a synchrotron XRF study. *Phys. Med. Biol.* **47**, 2327–2339. (doi:10.1088/0031-9155/47/13/310)

Geraki, K., Farquharson, M. J. & Bradley, D. A. 2004 X-ray fluorescence and energy dispersive diffraction for the quantification of elemental concentrations in breast tissue. *Phys. Med. Biol.* **49**, 99–110. (doi:10.1088/0031-9155/49/1/007)

Hall, C., Barnes, P., Cockcroft, J. K., Colston, S. L., Hausermann, D., Jacques, S. D. M., Jupe, A. C. & Kunz, M. 1998 Synchrotron energy-dispersive X-ray diffraction tomography. *Nucl. Instrum. Methods Phys. Res. Sect. B: Beam Interact. Mater. Atom* **140**, 253–257. (doi:10.1016/S0168-583X(97)00994-4)

Harding, G. & Schreiber, B. 1999 Coherent X-ray scatter imaging and its applications in biomedical science and industry. *Radiat. Phys. Chem.* **56**, 229–2545. (doi:10.1016/S0969-806X(99)00283-2)

Harding, G., Newton, M. & Kosanetzky, J. 1990 Energy-dispersive X-ray-diffraction tomography. *J. Phys. Med. Biol.* **35**, 33–41. (doi:10.1088/0031-9155/35/1/004)

Honemaki, V., Sleight, J. & Suortii, P. 1990 Characteristic X-ray flux from sealed Cr, Cu, Mo, Ag and W tubes. *J. Appl. Cryst.* **23**, 412–417. (doi:10.1107/S0021889890006082)

Kay, M. I., Young, R. A. & Posner, A. S. 1964 Crystal structure of hydroxyapatite. *Nature* **204**, 1050–1052. (doi:10.1038/2041050a0)

Kern, A. A. & Coelho, A. A. 1998 *A new fundamental parameters approach in profile analysis of powder data*, pp. 144–151. Delhi, India: Allied Publishers Ltd.

Korsunsky, A. M., Collins, S. P., Owen, R. A., Daymond, M. R., Achtioui, S. & James, K. E. 2002 Fast residual stress mapping using energy dispersive X-ray diffraction on station 16.3 at the SRS. *J. Synchrotron Radiat.* **9**, 77–81. (doi:10.1107/S0909049502001905)

Lewis, R. A. *et al.* 2000 Breast cancer diagnosis using scattered X-rays. *J. Synchrotron Radiat.* **7**, 348–352. (doi:10.1107/S0909049500009973)

McGann, W., Raynam, K. & Ribiero, N. 1993 US patent 5263075, 16 November 1993.

Seller, P., Gannon, W. J., Holland, A. D., Iles, G., Lowe, B. G., Prydderch, M. L., Thomas, S. L. & Wade, R. 1998 Silicon pixel detector for X-ray spectroscopy. In *SPIE, EUV, X-ray and Gamma-ray Instrumentation for Astronomy IX, July 1998, San Diego, CA, USA*, vol. 3445.

Tunna, L., Barclay, P., Cernik, R. J., Khor, K. H., O'Neill, W. & Seller, P. 2006 The manufacture of a very high precision x-ray collimator array for rapid tomographic energy dispersive diffraction imaging (TEDDI). *Meas. Sci. Technol.* **17**, 1767–1775. (doi:10.1088/0957-0233/17/7/015)